Effect of Electrostatic Interactions on Phase Stability of Cubic Phases of Membranes of Monoolein/Dioleoylphosphatidic Acid Mixtures

Shu Jie Li ,* Yuko Yamashita,† and Masahito Yamazaki*†
*Materials Science, Graduate School of Science and Engineering, and †Department of Physics, Faculty of Science, Shizuoka University, Shizuoka 422-8529, Japan

ABSTRACT To elucidate effects of electrostatic interactions resulting from surface charges on structures and phase stability of cubic phases of lipid membranes, membranes of 1-monoolein (MO) and dioleoylphosphatidic acid (DOPA) (DOPA/MO membrane) mixtures have been investigated by small-angle x-ray scattering method. As increasing DOPA concentration in the DOPA/MO membrane at 30 wt% lipid concentration, a phase transition from Q^{224} to Q^{229} phase occurred at 0.6 mol% DOPA, and at and above 25 mol% DOPA, DOPA/MO membranes were in the L_α phase. As NaCl concentration in the bulk phase increased, for 10% DOPA/90% MO membrane in excess water, a Q^{229} to Q^{224} phase transition occurred at 60 mM NaCl, and then a Q^{224} to H_{II} phase transition occurred at 1.2 M NaCl. Similarly, for 30% DOPA/70% MO membrane in excess water, at low NaCl concentrations it was in the L_α phase, but at and above 0.50 M NaCl it was in the Q^{224} phase, and then at 0.65 M NaCl a Q^{224} to H_{II} phase transition occurred. These results indicate that the electrostatic interactions in the membrane interface make the Q^{229} phase more stable than the Q^{224} phase, and that, at larger electrostatic interactions, the L_α phase is more stable than the cubic phases (Q^{224} and Q^{229}). We have found that the addition of tetradecane to the MO membrane induced a Q^{224}-to-H_{II} phase transition and also that to the 30% DOPA/70% MO membrane induced an L_α-to-H_{II} phase transition. By using these membranes, the effect of the electrostatic interactions resulting from the membrane surface charge (DOPA) on the spontaneous curvature of the monolayer membrane has been investigated. The increase in DOPA concentration in the DOPA/MO membrane reduced the absolute value of spontaneous curvature of the membrane. In the 30% DOPA/70% MO membrane, the absolute value of spontaneous curvature of the membrane increased with an increase in NaCl concentration. On the basis of these new results, the phase stability of DOPA/MO membranes can be reasonably explained by the spontaneous curvature of the monolayer membrane and a curvature elastic energy of the membrane.

INTRODUCTION

Cubic phases of lipid membranes have attracted much attention in both biological and physicochemical aspects (Luzzati and Husson, 1962; Gruner et al., 1985; Lindblom and Rilfors, 1989; Seddon and Templer, 1995; Luzzati et al., 1997). So far, many kinds of cubic phases, such as Q^{224}, Q^{229}, Q^{230}, Q^{225}, Q^{223}, Q^{227}, Q^{212}, have been found in lipids extracted from cells and also pure lipids in water by x-ray diffraction and freeze-fracture electron microscopy. They have been postulated to play several important biological roles in biomembranes, such as membrane fusions, a control of functions of membrane proteins, and ultrastructural organizations inside cells (Luzzati, 1997; Colotto et al., 1996; Basáñez et al., 1996; de Kruijff, 1997; Colotto and Epand, 1997). Recently, it was elegantly shown that the cubic phases are also very useful for crystallization of membrane proteins (Landau and Rosenbush, 1996; Pebay-Peyroula et al., 1997; Rummel et al., 1998). Understanding of stability of cubic phases has also been an important subject in the field of the lipid polymorphism, but the mechanism of the stability is not well understood yet (Anderson et al., 1988; Luzzati et al., 1997; Seddon and Templer, 1995). Especially, elucidation of the mechanism of phase transitions between different cubic phases and also between cubic phases and other phases, such as liquid–crystalline (L_α) and inverted hexagonal (H_{II}), is essential for various other researches of the dynamics of biomembranes, such as the membrane fusion and development of a new crystallization technique.

One family of cubic phases, i.e., Q^{224}, Q^{229}, and Q^{230}, has an infinite periodic minimal surface (IPMS) consisting of bicontinuous regions of water and hydrocarbon (Seddon and Templer, 1995; Andersson et al., 1988). In these cubic phase membranes, the minimal surface is located at the bilayer midplane, which is the interface of two monolayer membranes (Gruner, 1989), and the minimal surface has a negative Gaussian curvature and zero mean curvature at all points. Several physicochemical studies on these cubic phases, such as determination of temperature–water concentration phase diagrams and lateral diffusion of lipids, have been done. Especially, the temperature–water concentration phase diagram of 1-monoolein (MO) (C18:1), a typical monoacylglycerol, has been extensively investigated (Longley and McIntosh, 1983; Hyde et al., 1984; Caffrey, 1987; Czeslik et al., 1995; Briggs et al., 1996; Qiu and Caffrey, 2000). Figure 1 shows an equilibrium phase diagram of MO (Qiu and Caffrey, 2000). In excess water, the MO membrane is in the Q^{224} phase (space group Pn3m) at wide temperature range. Several kinds of lipids, such as DDPE (didodecyl phosphatidylethanolamine) (Seddon et al., 1990), monoelaidin, and also lipid extracts from *Sulfolobus*

Received for publication 23 October 2000 and in final form 28 April 2001.
Address reprint requests to Dr. Masahito Yamazaki, Department of Physics, Faculty of Science, Shizuoka University, 836 Oya, Shizuoka 422-8529, Japan. Tel.: 81-54-238-4741; Fax: 81-54-238-4741; E-mail: spmyama@ipc.shizuoka.ac.jp.

0006-3495/01/08/983/11 $2.00

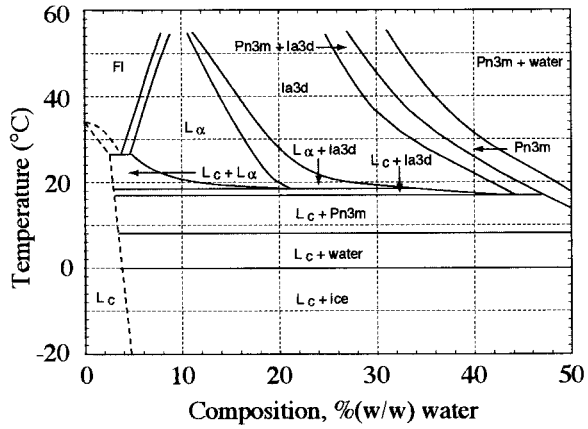

FIGURE 1 Equilibrium temperature–composition (water concentration) diagram for the MO/water system. This figure is reprinted from Qiu and Caffrey (2000) with permission from Elsevier Science and Dr. Caffrey.

solfataricius (Luzzati et al., 1987) form the Q^{224} phase. This cubic phase has an IPMS consisting of bicontinuous regions of water and hydrocarbon, which corresponds to Schwartz D surface (sometimes denoted the F-surface) (Seddon and Templer, 1995; Hyde et al., 1984). Two interwoven tetrahedral networks of rodlike water-channels are arranged on a double-diamond lattice. As shown in Fig. 1, in nonexcess water condition, as the water contents decrease, the MO membrane changes from Q^{224} (Pn3m) to Q^{230} phase (space group Ia3d; Schwartz G surface), and then to L_α phase at wide temperature range (20~50°C). This effect of water contents on the phase stability of cubic phases of the MO membrane has been explained by the curvature elastic energy (Chung and Caffrey, 1994b). In contrast, several substances can change the stability of the Q^{224} phase of the MO membrane. Cytochrome C (Mariani et al., 1988) and oleic acid (Aota-Nakano et al., 1999) can induce Q^{229} phase (space group Im3m; Schwartz P surface) in the MO membrane in excess water. A nonionic detergent, *n*-dodecyl-β-D-maltopyranoside, can induce Q^{230} (Ia3d) phase in the MO membrane (Ai and Caffrey, 2000). However, the phase stability and the structure determinant of the Q^{224} phase are still not well understood.

In our previous report, membranes of MO and oleic acid (OA) mixtures (OA/MO membrane) have been investigated by small-angle x-ray scattering method (SAXS) (Aota-Nakano et al., 1999). We found that, as OA concentration in the OA/MO membrane in neutral pH increased, a phase transition from Q^{224} to Q^{229} phase occurred, and, above 1.0 mol% OA (less than 15 mol%), the OA/MO membranes were in the Q^{229} phase. Moreover, when NaCl concentration in the bulk phase was large, the Q^{224} phase was more stable than the Q^{229} phase in the OA/MO membranes containing high concentrations of OA. These results indicate that the electrostatic interactions make the Q^{229} phase more stable than the Q^{224} phase. However, we could not investigate effects of high surface-charge density of the membrane on the phase stability because of the experimental difficulty that made the previous report incomplete. We also reported that these results could be explained in terms of the spontaneous curvature of the monolayer membrane, although we didn't have any experimental evidence on the effect of the surface charge of the membrane on the spontaneous curvature.

In this report, we have investigated in detail the effect of electrostatic interactions due to the surface charges on structures and phase stability of the cubic phase of the MO membrane by SAXS. To change the surface charge density in the MO membrane, we added various amounts of dioleoylphosphatidic acid (DOPA) into the MO membrane from 0 to 40 mol% DOPA. We have found that, as the DOPA concentration increases, a phase transition from Q^{224} to Q^{229} phase occurred in DOPA/MO membrane, and, at higher DOPA concentration (≥25 mol%), the DOPA/MO membranes were in the L_α phase. However, as NaCl concentration in the bulk phase increases, the phase of the MO membrane changes from L_α to Q^{224}, then to H_{II} phase in the DOPA/MO membranes. Next, we have found that the addition of tetradecane to the MO membrane induced the cubic (Q^{224})-to-H_{II} phase transition, and also to the 30% DOPA/70% MO membrane induced the L_α-to-H_{II} phase transition. By using these membranes, effects of the electrostatic interactions due to the membrane surface charge on the spontaneous curvature of the monolayer membrane has been investigated. Our results show that the absolute value of the spontaneous curvature decreased with an increase in the electrostatic interactions. Based on these new results, we have discussed the mechanism of these phase transitions and the phase stability of the cubic phase of the DOPA/MO membrane in terms of the spontaneous curvature of the monolayer membrane and the curvature elastic energy of the membrane. We can conclude that the electrostatic interactions and also steric repulsion between the lipid headgroups play an important role on the phase stability of cubic phases.

MATERIALS AND METHODS

Materials and sample preparation

MO (1-monooleoyl-rac-glycerol) and tetradecane were purchased from Sigma Chemical Co. (St. Louis, MO). DOPA sodium salt was purchased from Avanti Polar Lipid (Alabaster, AL). They were used without further purification.

Lipid dispersions were prepared as follows. Appropriate amounts of 10 mM PIPES buffer (pH 7.0) containing a given concentration of NaCl were added to dry lipids, i.e., mixture of MO and DOPA, in excess water (~7 wt% lipids) condition or at 30 wt% lipid concentration. Then, the suspensions were vortexed for about 30 s at room temperature (~25°C) several times. For measurements of x-ray diffraction, pellets after centrifugation (13,000 × *g*, 30 min at 20°C; Tomy, MR-150) of the lipid suspensions were used.

To investigate structures of DOPA/MO membranes containing 16 wt% tetradecane, we used almost the same method of Chen and Rand (1997, 1998) as follows. All procedures were done at room temperature (~25°C). The appropriate amount of MO containing various concentrations of DOPA in chloroform was dried by N_2, and then under vacuum by rotary

pump for more than 12 hrs. Tetradecane was added to the dry lipid by weighing directly, and then vortexed for about 30 s several times. After 48 hrs incubation for equilibration, the appropriate amount of 10 mM PIPES buffer (pH 7.0) containing a given concentration of NaCl was added to this dry-lipid/tetradecane mixture in excess solvents, and the suspension was vortexed for about 30 s several times. Then, it was incubated for another 48 hrs for equilibration. For measurement of x-ray diffraction, the precipitation of the suspensions after the vortex without centrifugation were used.

X-ray diffraction

X-ray diffraction experiments were performed by using Nickel-filtered Cu K_α x-ray ($\lambda = 0.154$ nm) from a rotating anode-type x-ray generator (RU-300 Rotaflex, Rigaku, Tokyo, Japan) at the operating condition (40 kV × 200 mA). SAXS data were recorded using a linear (one-dimensional) position-sensitive proportional counter (Rigaku) (Glatter and Kratky, 1982) with camera length of 350 mm and associated electronics (multichannel analyzer, etc., Rigaku). In all cases, samples were sealed in a thin-walled glass capillary tube (outer diameter 1.0 mm) and mounted in a thermostatable holder whose stability was ±0.2°C (Yamazaki et al., 1992).

Formation and observation of giant unilamellar vesicle

DOPA/MO-giant unilamellar vesicles (GUVs) were prepared as follows. 200 μl of 1 mM phospholipids (a mixture of DOPA and MO) in chloroform in a small glass vessel was dried by a stream of nitrogen gas at room temperature. Then, residual solvent was completely removed by rotary vacuum pump for more than 12 hrs. A small amount of water (about 10 μl) was added in this glass vessel, and incubated at 45°C for a few minutes (pre-hydration). Then, 1 ml 10 mM PIPES buffer (pH 7.0) was added in this vessel and incubated at 37°C for 2 hrs.

A 10-μl GUV solution was diluted into 200 μl 10 mM PIPES buffer (pH 7.0), and then the solution was put into a hand-made microchamber. The chamber (1 × 1 cm wide and 3 mm high, internal volume ~0.3 ml) was formed on the slide glass by placing on it a U-shaped silicone-rubber spacer. We observed GUVs under an inverted Hoffman modulation-contrast microscope (IX-70, Olympus, Tokyo, Japan). In most cases, GUVs were observed at room temperature. Hoffman modulation-contrast images of GUVs were recorded through a CCD camera (DXC-108, SONY, Tokyo, Japan) on a video recorder (HR-VR108, Victor, Tokyo, Japan).

RESULTS

Effect of DOPA concentration on structures of DOPA/MO membranes

We have investigated effects of DOPA concentration (mol%) in DOPA/MO membranes on their structures in 10 mM PIPES buffer (pH 7.0) in excess water condition at 20°C by the SAXS method. It is well known that the MO membrane in excess water at 20°C is in the Q^{224} phase. Addition of small amounts of DOPA into the MO membrane changed this cubic structure. The SAXS pattern of 0.3% DOPA/99.7% MO membrane was similar to that of 100% MO membrane (Fig. 2*a*). Several peaks had spacings in the ratio of $\sqrt{2}:\sqrt{3}:\sqrt{4}:\sqrt{6}:\sqrt{8}:\sqrt{9}:\sqrt{10}:\sqrt{11}:\sqrt{12}$, indexed as (110), (111), (200), (211), (220), (221), (310), (311), and (222) reflections (Fig. 3). This corresponds to a primitive cubic phase of space group Pn3m (Q^{224}) (cubic aspect #4) (International Tables for X-ray Crystallography, 1985). The reflections of $\sqrt{10}$ and $\sqrt{11}$ were very small, which is the same as that of the Q^{224} phase of the 100% MO membrane (Caffrey, 1987). The reciprocal spacing, S, of the cubic phase is connected with the lattice constant, a, by $S(h, k, l) = (1/a) \cdot (h^2 + k^2 + l^2)^{1/2}$, where h, k, and l are Miller indices (Seddon and Templer, 1995). The lattice constant, a, (here, we call it the structure parameter to use this word for different kinds of phases) of this 0.3% DOPA/99.7% MO membrane, determined by the gradient of the plot in Fig. 3, was 10.7 nm. It was a little larger than that of the 100% MO membrane (Fig. 4). In contrast, in the SAXS pattern of 2.0% DOPA/98% MO membrane, several peaks had spacings in the ratio of $\sqrt{2}:\sqrt{4}:\sqrt{6}:\sqrt{8}:\sqrt{10}:\sqrt{12}:\sqrt{14}:\sqrt{16}:\sqrt{18}:\sqrt{20}:\sqrt{22}:\sqrt{24}$ (Fig. 2 *b*). They were indexed as (110), (200), (211), (220), (310), (222), (321), (400), (411), (420), (332), and (422) reflections on a body-centered cubic phase of space group Im3m (Q^{229}) (cubic aspect #8) (International Tables for X-ray Crystallography, 1985). The reflection of $\sqrt{16}$ was very small. The lattice

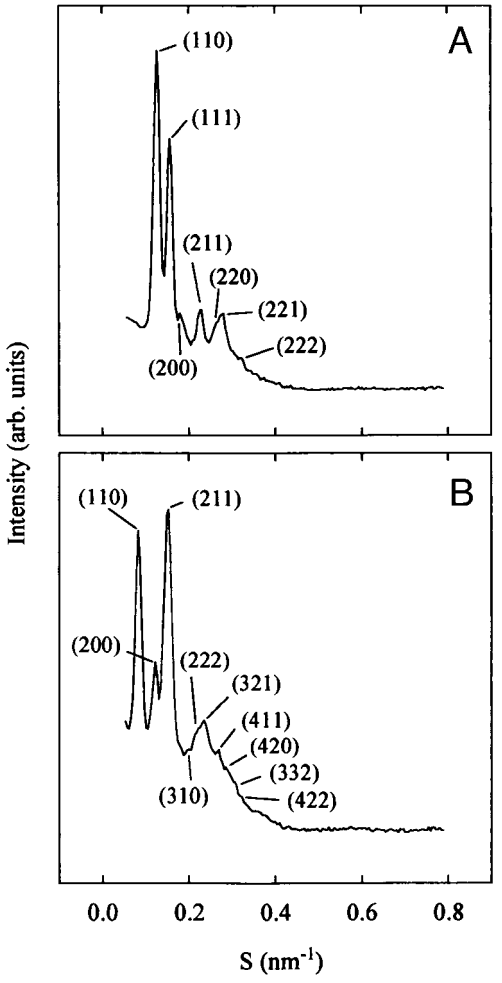

FIGURE 2 X-ray diffraction profile of (*A*) 0.3% DOPA/99.7% MO membrane and (*B*) 2.0% DOPA /98% MO membrane in 10 mM PIPES buffer (pH 7.0) at 20°C.

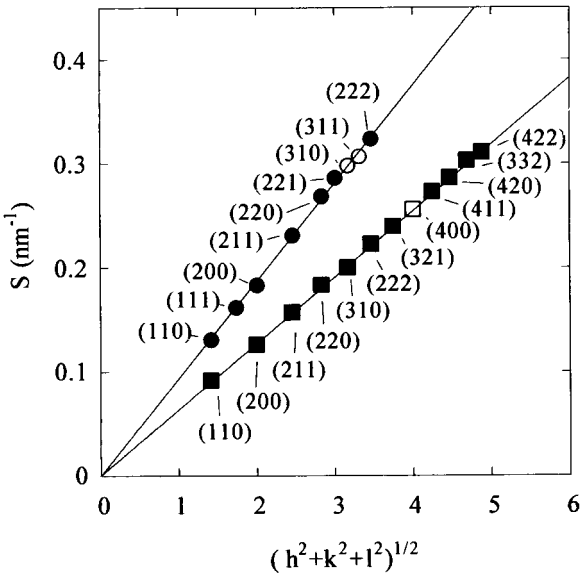

FIGURE 3 Indexing of the x-ray diffraction (SAXS) data of the 0.3% DOPA/99.7% MO membrane (●) and 2.0% DOPA/98% MO membrane (■) in 10 mM PIPES buffer (pH 7.0) at 20°C. The open symbols (○, □) show reflections, which, although allowed by the space group, were not clearly observed due to weak intensities.

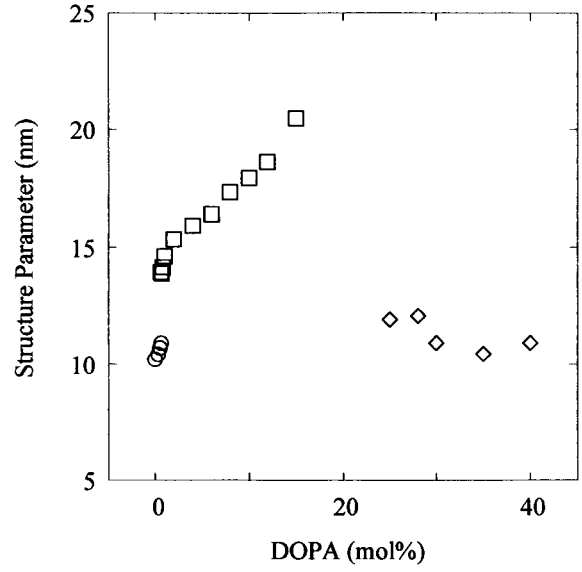

FIGURE 5 The structure parameter of DOPA/MO membranes containing various concentrations of DOPA (mol%) in 10 mM PIPES buffer (pH 7.0) at 30 wt% lipid condition at 20°C determined by SAXS. ○, Q^{224} phase; □, Q^{229}; ◇, L_α phase.

constant of this Q^{229} phase was 15.7 nm (Fig. 3). Figure 4 shows the dependence of the lattice constant and kind of cubic phase on the contents of DOPA in DOPA/MO membranes. Less than 0.5% DOPA, DOPA/MO membranes were in the Q^{224} phase. At 0.5% DOPA, a phase transition from Q^{224} to Q^{229} phase occurred, and, above 0.5% DOPA, DOPA/MO membranes were in the Q^{229} phase. At 0.5% DOPA, both the Q^{224} and Q^{229} phases coexisted, and the lattice constant for the Q^{224} and Q^{229} phase were 10.9 and 13.6 nm, respectively. The ratio of the lattice constant (Q^{229}/Q^{224}) was 1.25, which is close to the theoretical value (1.28) determined by the analysis of the coexisting cubic phases based on the Bonnet transformation (Hyde et al., 1984; Tenchov et al., 1998). The lattice constant of the membranes gradually increased with an increase in DOPA concentrations. Above 12% DOPA, peaks in SAXS pattern became broad, and thereby difficult to analyze.

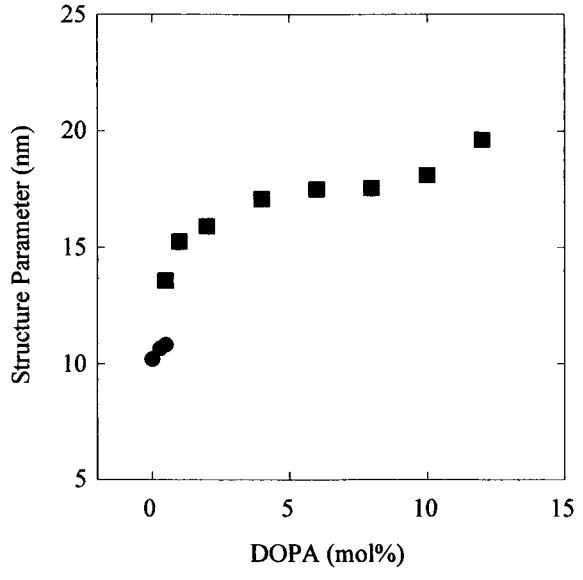

FIGURE 4 The structure parameter, i.e., the lattice constant *a* of cubic phases of DOPA/MO membranes containing various concentrations of DOPA (mol%) in 10 mM PIPES buffer (pH 7.0) in excess water condition at 20°C determined by SAXS. ●, Q^{224} phase; ■, Q^{229} phase.

To elucidate effects of high concentrations of DOPA in the DOPA/MO membranes, we have investigated structures of DOPA/MO membranes at high lipid concentrations (30 wt% lipids) in 10 mM PIPES buffer (pH 7.0). Figure 5 shows a detailed dependence of the spacing and structure of DOPA/MO membrane on DOPA concentration (mol%). SAXS patterns of the DOPA/MO membranes containing less than 13% DOPA under this condition were almost the same as those in excess water. At 0.6% DOPA, a phase transition from Q^{224} to Q^{229} phase occurred, and both the phases coexisted, where the ratio of the lattice constant (Q^{229}/Q^{224}) was 1.27. The lattice constant of the DOPA/MO membrane in the Q^{229} phase gradually increased from 14.6 to 20.5 nm with an increase in DOPA concentration from 1.0 to 15%. At 16~24% DOPA, it was difficult to specify the phase. At and above 25% DOPA, a new set of SAXS peaks appeared with a large spacing (11.3 ± 0.5 nm) in the ratio of 1:2:3 (Fig. 6), which is consistent with an L_α phase. The spacing (i.e., the structure parameter) of the L_α phase was almost constant with an increase in DOPA concentration from 25 to 40% (Fig. 5). The

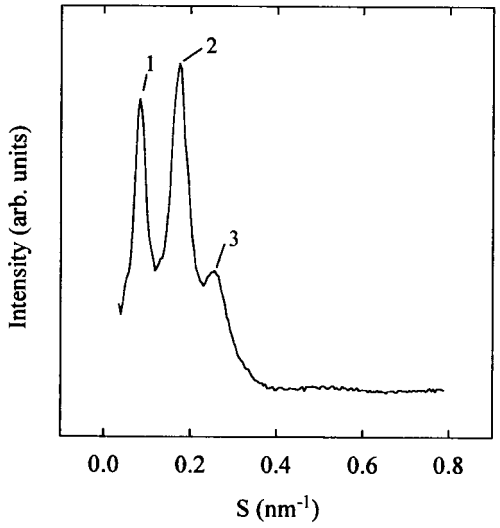

FIGURE 6 X-ray diffraction profile of 40% DOPA/60% MO membrane in 10 mM PIPES buffer (pH 7.0) at 30 wt% lipid condition at 20°C. The spacing of L_α phase is 11.4 nm.

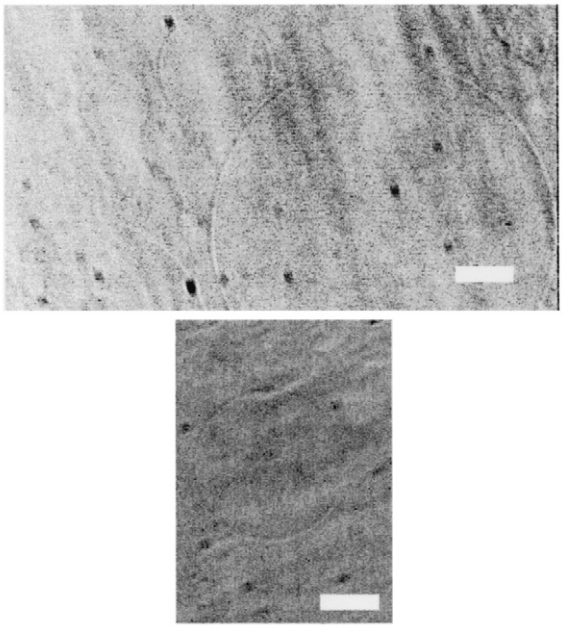

FIGURE 7 Hoffman modulation contrast image of a GUV of 30% DOPA/70% MO GUV prepared in 10 mM PIPES buffer (pH 7.0). Scale bar: 20 μm.

condition of these membranes in the L_α phase was not in excess water, because the intermembrane distance of the DOPA/MO-multilamellar vesicle was very large as a result of the electrostatic repulsion between the membranes. Therefore, the spacing did not change as the DOPA concentration increased.

To confirm the formation of the L_α phase in DOPA/MO membranes containing high concentration of DOPA in excess water, we have tried to make a GUV of these membranes. Figure 7 shows a Hoffman modulation contrast image of 30% DOPA/70% MO GUV prepared in 10 mM PIPES buffer (pH 7.0). In most cases, these GUVs were spherical vesicles with 20~50 μm diameter. This result indicates that the DOPA/MO membranes containing high concentration of DOPA in excess water were in the L_α phase, and thereby they can form the GUVs. It supports the above conclusion based on the SAXS experiments.

Effect of salt concentration on the lattice constants and kinds of cubic phase in DOPA/MO membranes

To elucidate effects of the electrostatic interactions on the phase stability and the lattice constant of DOPA/MO membranes, we have investigated dependence of NaCl concentration in the bulk phase on structures of these membranes in excess water. As shown in Fig. 4, 10% DOPA/90% MO membrane in 10 mM PIPES buffer (pH 7.0) was in the Q^{229} phase, and the same membrane in the same buffer containing 0.1 M NaCl was in the Q^{224} phase (Fig. 8 *a*). Figure 8 *b* shows that, in the 10% DOPA/90% MO membrane in the presence of 1.6 M NaCl, several peaks in the SAXS pattern had spacing in the ratio of $1:\sqrt{3}:2$, corresponded to the (10), (21), and (20) reflections on a 2-dimensional inverted hexagonal (H_{II}) phase. The basis vector length of this H_{II} phase (center-to-center distance of adjacent cylinders; here we call it the structure parameter), d, calculated by $d = (2/\sqrt{3})x$ (where x is the spacing in the SAXS pattern), was 6.7 nm. Figure 9 shows a detailed dependence of the structure parameter and kinds of phase of this membrane on NaCl concentration. At less than 60 mM NaCl, they were in the Q^{229} phase. At 60 mM NaCl, a phase transition from Q^{229} to Q^{224} phase occurred, and at 60 and 70 mM NaCl, both the phases coexisted, where the ratio of the lattice constant (Q^{229}/Q^{224}) was 1.31, which is close to the theoretical value. The lattice constant of the Q^{224} phase gradually decreased with an increase in NaCl concentration. At 1.2 M NaCl, a phase transition from Q^{224} to H_{II} phase occurred, and, above 1.5 M NaCl, the 10% DOPA/90% MO membrane was in the H_{II} phase.

Next, we have investigated dependence of NaCl concentration on structures of 30% DOPA/70% MO membrane in excess water. As the previous data show, in 0 M NaCl, it was in the L_α phase (Fig. 6 and Fig. 7). In the presence of low NaCl concentration below 0.37 M, after the centrifugation of the samples, pellets were not observed, and the SAXS measurement of the suspension gave a broad peak that was difficult to analyze. However, judging from the analysis of the membrane in 0 M NaCl in the previous section, we consider that these membranes were in the L_α phase. At and above 0.50 M NaCl (less than 0.75 M NaCl), the SAXS pattern showed that the membranes were in the Q^{224} phase and that the lattice constant of the Q^{224} phase

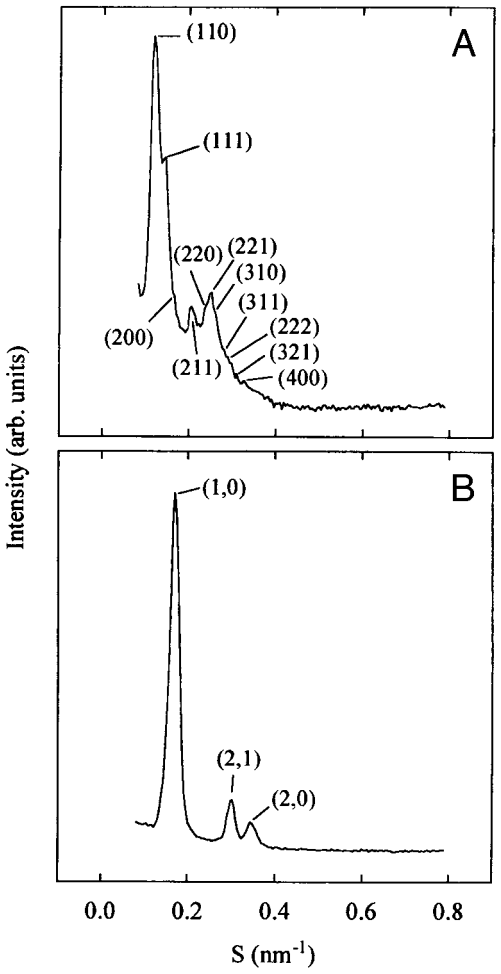

FIGURE 8 X-ray diffraction profile of 10% DOPA/90% MO membrane in (*A*) 10 mM PIPES buffer (pH 7.0) containing 0.1 M NaCl and (*B*) 10 mM PIPES buffer (pH 7.0) containing 1.6 M NaCl at 20°C.

gradually decreased with an increase in NaCl concentration (Fig. 10). At the intermediate concentration (0.37 M $\leq$ NaCl $<$ 0.50 M), there were several peaks in SAXS pattern. They contained peaks due to both the L_α phase and the cubic phase, which could not be indexed with reliability. At 0.65 M NaCl, a phase transition from Q^{224} to H_{II} phase occurred, and at and above 0.75 M NaCl, the 30%-DOPA/70%-MO membranes were in the H_{II} phase.

Spontaneous curvature of DOPA/MO membranes

To consider the mechanism of these phase transitions, we have investigated effects of DOPA concentration and NaCl concentration in the bulk phase on the spontaneous curvature of MO membrane. To allow the lipid membranes in the H_{II} phase to express the spontaneous curvature, H_0, the addition of alkanes such as decane and tetradecane to the membranes is required because they fill the interstitial region of the H_{II} phase and relax the alkyl chain packing stress (Gruner, 1985; Rand et al., 1990; Chen and Rand, 1998). At first, we investigated the effect of the concentration of tetradecane in the membrane on the structure of the MO membrane in excess water at 20°C in 10 mM PIPES buffer (pH 7.0). Above 8%(w/w) tetradecane, the MO membranes were in the H_{II} phase (data not shown). Therefore, to get information of the dependence of the spon-

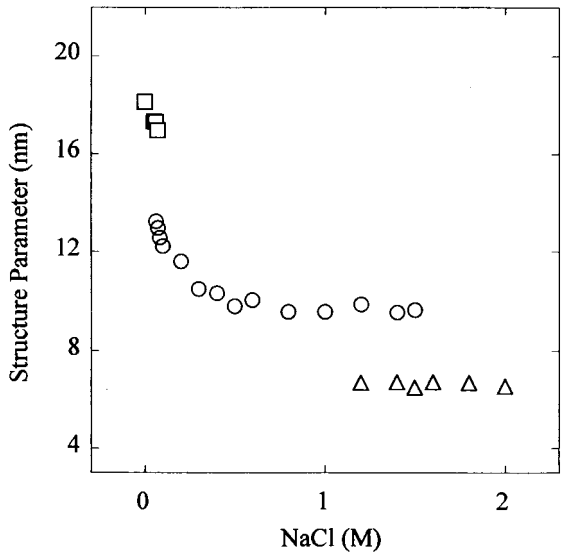

FIGURE 9 The structural parameter (i.e., the lattice constant *a* of cubic phases and the basis vector length *d* of the H_{II} phase) of the 10% DOPA/90% MO membranes in 10 mM PIPES buffer (pH 7.0) containing various concentrations of NaCl (M) at 20°C determined by SAXS. ○, Q^{224} phase; □, Q^{229} phase; Δ, H_{II} phase.

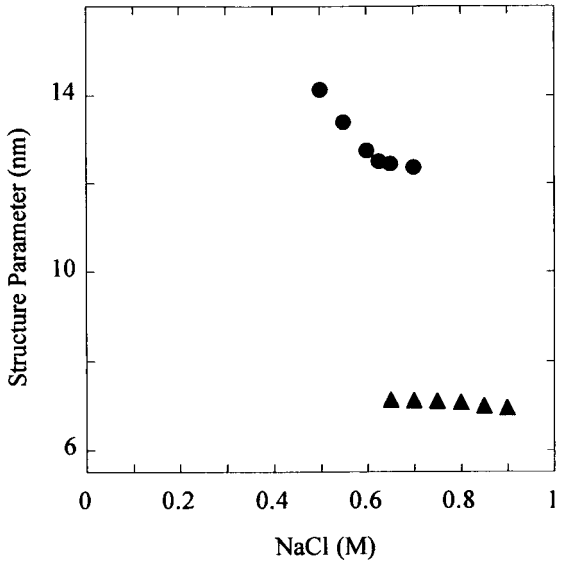

FIGURE 10 The structural parameter (i.e., the lattice constant *a* of cubic phases and the basis vector length *d* of the H_{II} phase) of the 30% DOPA/70% MO membranes in 10 mM PIPES buffer (pH 7.0) containing various concentrations of NaCl (M) at 20°C determined by SAXS. ●, Q^{224} phase; and ▲, H_{II} phase.

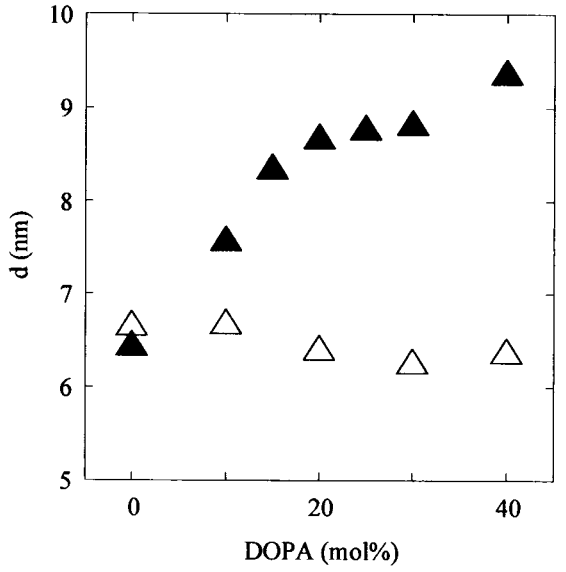

FIGURE 11 The basis vector length, d, of H_{II} phases of DOPA/MO membrane containing 16 wt% tetradecane versus DOPA (mol%) concentration in 10 mM PIPES buffer (pH 7.0) in excess water at 20°C determined by SAXS. ▲, in 0 M NaCl; Δ, in 1.0 M NaCl.

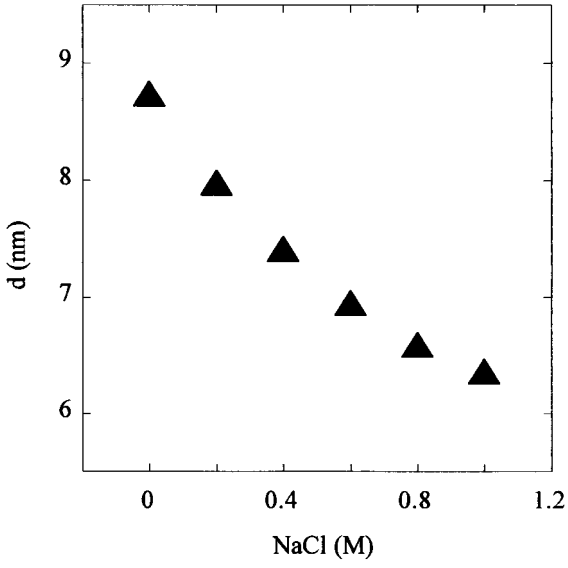

FIGURE 12 The basis vector length, d, of H_{II} phases of 30% DOPA/70% MO membrane containing 16wt% tetradecane in 10 mM PIPES buffer (pH 7.0) versus NaCl concentration (M) in excess water at 20°C determined by SAXS.

taneous curvature of the MO membrane on DOPA concentration, we investigated the structure of the DOPA/MO membrane containing 16 wt% tetradecane in excess water at 20°C (Fig. 11). The basis vector length, d, of the DOPA/MO/tetradecane membrane in 10 mM PIPES buffer (pH 7.0) gradually increased from 6.5 to 9.4 nm with an increase in DOPA concentration from 0 to 40 mol%. In contrast, the basis vector length, d, of the DOPA/MO/tetradecane membrane in 10 mM PIPES buffer (pH 7.0) containing 1.0 M NaCl gradually decreased from 6.7 to 6.2 nm with an increase in DOPA concentration from 0 to 30 mol%.

We also investigated the structure of 30% DOPA/70% MO membrane containing 16 wt% tetradecane in 10 mM PIPES buffer (pH 7.0) containing various NaCl concentrations (Fig. 12). In 0 M NaCl, the 30% DOPA/70% MO membrane without tetradecane was in the L_α phase (Fig. 6 and Fig. 7), but the 30% DOPA/70% MO membrane containing 16 wt% tetradecane was in the H_{II} phase. As shown in Fig. 12, d of the 30% DOPA/70% MO/tetradecane membrane in excess water gradually decreased from 8.7 to 6.4 nm with an increase in NaCl concentration from 0 M to 1.0 M.

DISCUSSION

The effect of electrostatic interactions on phase stability and structure of DOPA/MO membranes

The results of x-ray diffraction experiments clearly show that, in DOPA/MO membranes in excess water at neutral pH, the Q^{229} phase is more stable than the Q^{224} phase when the surface charge density due to the DOPA is relatively high and salt concentration in the bulk phase is low. Under this condition, the electrostatic interactions due to the surface charges of these membranes are large. Therefore, we can say that these electrostatic interactions in the membrane interface increase the stability of the Q^{229} phase with respect to that of the Q^{224} phase. This is the same conclusion as that of OA/MO membranes in excess water (Aota-Nakano et al., 1999). When the DOPA concentration is higher and thereby the electrostatic interactions become larger, the L_α phase becomes more stable than the Q^{229} phase. The formation of the DOPA/MO-GUV supports this fact. In the case of OA/MO membrane in excess water, this situation would be the same, but we could not identify the phase of the OA/MO membranes containing a high concentration of OA because of experimental difficulty (Aota-Nakano et al., 1999). This effect of the electrostatic interactions on the phase stability of the DOPA/MO membrane can be considered as follows.

Spontaneous curvature of DOPA/MO membranes

The spontaneous (or intrinsic) curvature of a single monolayer membrane, H_0, is a useful parameter characterizing nonbilayer membranes, and expressed as $H_0 = 1/R_0$, where R_0 is the radius of spontaneous curvature (Gruner, 1985; 1989; Marsh, 1996). Inverted curved structures such as the H_{II} phase, where the spontaneous curvature of the monolayer is toward the water region, have large negative H_0 values. In contrast, normal structures such as micelles, where the spontaneous curvature of the monolayer is toward the alkyl chain region, have large positive H_0 values. The spontaneous curvature of a single

monolayer membrane is defined as its radius of curvature to minimize the curvature elastic energy of the monolayer membrane, which is determined by physical properties of the monolayer by itself without the interaction of other monolayer membrane (Gruner, 1985; 1989; Marsh, 1996). Therefore, it is a kind of an ideal curvature of the monolayer membrane. In most cases, it is difficult for the lipid membrane to have the spontaneous curvature, because the interaction between two monolayer membranes also plays an important role in the determination of its curvature. The determinant of the spontaneous curvature of the single monolayer membrane is a geometric packing of the constituent lipids. It is characterized by a packing parameter, V/Al, where V is the volume of the entire lipid molecule, A the area of the lipid headgroup at the lipid–water interface, and l its length (Marsh, 1996). Values for these parameters (V, A, l) depend not only on the molecular structure of lipids but also on external conditions such as temperature and solvents (including salts), because these external conditions largely change the optimal values of these parameters (Marsh, 1996; Kinoshita et al., 2001). Therefore, the spontaneous curvature of the monolayer membrane depends on both the molecular structure of the constituent lipids and various external conditions, which has been verified by experiments (Marsh, 1996; Kinoshita et al., 2001).

We have a useful method to get information of the spontaneous curvature of the lipid membrane. To allow the lipid monolayer membranes in the H_{II} phase in excess water to express the spontaneous curvature, the addition of alkanes such as decane and tetradecane to the membranes is required, because they fill the interstitial region of the H_{II} phase and relax the alkyl chain packing stress (Gruner, 1985, 1989; Rand et al., 1990; Chen and Rand, 1998). Under this condition, the curvature of the monolayer membrane in the H_{II} phase is very close to the spontaneous curvature. We have found that the addition of tetradecane to the MO membrane induced the cubic (Q^{224})-to-H_{II} phase transition, and to the 30% DOPA/70% MO membrane induced the L_α-to-H_{II} phase transition. By using these membranes, we have investigated the effect of the electrostatic interactions due to the membrane surface charge (DOPA) on the spontaneous curvature H_0 of the single monolayer membrane. The result of Fig. 11 gives information on the change of the radius of spontaneous curvature R_0 of the DOPA/MO/tetradecane membrane in 10 mM PIPES buffer (pH 7.0). The basis vector length of the H_{II} phase, d, is expressed as a sum of the radius to the neutral plane (or pivotal plane or neutral surface), R_{pp}, and the distance between the bilayer midplane and the neutral plane, ξ, i.e., $d = 2(R_{pp} + \xi)$ (Gruner 1989; Rand et al., 1990; Turner et al., 1992; Templer et al., 1994). The neutral plane is the appropriate surface to define the curvature of the membrane, because the area of this plane keeps constant as the monolayer is bent. Experimentally, it is determined as the surface whose area does not change while water content varies, and is located at the alkyl chain region near the polar-apolar interface (Rand et al., 1990; Chung and Caffrey, 1994a; Rand and Fuller, 1994). In excess water, the DOPA/MO membrane containing 16 wt% tetradecane in the H_{II} phase has the spontaneous curvature, H_0, and thereby, $R_{pp} \approx R_0$. The increase in d of the DOPA/MO/tetradecane membrane induced by the increase in content of DOPA is attributed to the increase in R_{pp}, because the change in ξ is assumed to be small. Thus, the result of Fig. 11 shows that R_0 of the DOPA/MO membranes increases with an increase in DOPA concentration. It indicates that the increase in electrostatic interactions reduces the absolute value of spontaneous curvature, H_0, of the membrane to increase the average area of the lipid headgroup of the membrane. From this analysis and the result of Fig. 5, we can indicate that as the absolute value of spontaneous curvature, $|H_0|$, of the membrane decreases, the phase transition from Q^{224} to Q^{229} phase occurs, and then the Q^{229} to L_α phase transition occurs. Hence, the phase stability of these three phases is deeply correlated with the spontaneous curvature of the monolayer membrane. Similarly, the result of Fig. 12 shows that R_0 of the 30% DOPA/70% MO membranes decreased with an increase in NaCl concentration, indicating that, with a decrease in the electrostatic interactions, the absolute value of spontaneous curvature, $|H_0|$, of the membrane increases. Therefore, this result and Fig. 6 support the above hypothesis; as the absolute value of spontaneous curvature of the membrane decreases, the most stable phase changes from the Q^{224} to the L_α phase.

Moreover, at higher NaCl concentration, the H_{II} phase becomes most stable in the 30% DOPA/70% MO membranes. This result can be considered as follows. Other reports show that high concentration of NaCl stabilizes the H_{II} phase in the 100% MO membrane. However, at 20°C, it was in the Q^{224} phase in the presence of 0∼5 M NaCl (Caffrey, 1987). In contrast, in the 10% DOPA/90% MO membrane and the 30% DOPA/70% MO membrane, relatively low concentration of NaCl induced the H_{II} phase (i.e., 1.2 M and 0.65 M NaCl, respectively). Therefore, the effect of NaCl on the DOPA is larger than that on the MO, and the role of DOPA is more important for the phase stability of these DOPA/MO membranes at relatively low concentrations of NaCl. Fig. 11 also shows that R_o of the DOPA/MO membranes in 1.0 M NaCl decreased with an increase in DOPA concentration. It indicates that the presence of 1.0 M NaCl reduces the electrostatic interactions due to the surface charge of the membrane by the screening the electric potential, and the packing parameter of the DOPA (V/Al) under this condition is larger than that of MO. Thereby, $|H_0|$ of the DOPA/MO membrane in 1.0 M NaCl increases with an increase in DOPA concentration. Therefore, above the critical concentration of DOPA, the cubic-to-H_{II} phase transition occurs.

As described above, when the surface charge density of the membrane due to DOPA is high and the salt concentration in the bulk phase is low, $|H_0|$ is low. This is mainly due

to two kinds of electrostatic interactions. One is the repulsive electrostatic interaction between the headgroups, which may reduce $|H_0|$ to increase the distance between the headgroups. The other is the attractive electrostatic interaction between negative charge of the headgroup of DOPA and a dipole moment of water molecule. It attracts more water molecules near the headgroup, and thereby the effective volume of the headgroup increases, which may reduce $|H_0|$. Li and Schick (2000) showed that the latter electrostatic interaction induces a phase transition from H_{II} to L_α phase by theoretical calculation. We have also indicated by experiments that the latter electrostatic interaction is the prevailing one for the stability of the gel-phase dihexadecylphosphatidylcholine (DHPC) membrane in the presence of 0.5 M KCl (Furuike et al., 1999). The analysis of several experiments clearly show that the repulsive interaction between the headgroups of DHPC in the membrane at low pH, which have a net positive charge, is smaller than that of DHPC at neutral pH, where it does not have a net charge. This is due to the decrease in the steric repulsive interaction at low pH, because the protonation of the phosphate group (i.e., the loss of the negative charge) induces the decrease of water molecules near the phosphate group in the membrane interface (Furuike et al., 1999).

However, at present, we do not have enough experimental evidence to determine which electrostatic interaction is a dominant one to reduce $|H_0|$ of these liquid–crystalline DOPA/MO membranes at low ionic strength. Further study to elucidate this mechanism is necessary.

Phase stability of cubic phases

The difference of the chemical potential of the phospholipid membrane in the nonbilayer phase such as the cubic (Q^{224}, Q^{229}) phase and the H_{II} phase (μ^{nonbil}) and in the bilayer liquid–crystalline (L_α) phase (μ^{bil}), $\Delta\mu$, is expressed as (see e.g., Anderson et al., 1988; Gruner, 1989)

$$\begin{aligned}\Delta\mu &= \mu^{nonbil} - \mu^{bil}\\ &= (\mu^{nonbil}_{curv} - \mu^{bil}_{curv}) + (\mu^{nonbil}_{ch} - \mu^{bil}_{ch}) \qquad (1)\\ &= \Delta\mu_{curv} + \Delta\mu_{ch},\end{aligned}$$

where $\Delta\mu_{curv}$ is a term due to the curvature elastic energy (or curvature energy), and $\Delta\mu_{ch}$ is a term due to interstitial chain packing of the nonbilayer phase. The curvature elastic energy of the membrane, $\mu_{curv,}$ in Eq. 1 can be expressed as (Helfich, 1973; Gruner, 1989)

$$\mu_{curv} = 2\kappa\langle H - H_0\rangle^2 + \kappa_G\langle K\rangle, \qquad (2)$$

where κ is the elastic bending modulus, H the mean curvature, K the Gaussian curvature, κ_G the Gaussian curvature modulus, and $\langle\ \rangle$ means the average value over the area of the unit cell. The bicontinuous IPMS, such as the Q^{224} and the Q^{229} phase, has a negative Gaussian curvature, i.e., $K < 0$. It has zero mean curvature at all points in the bilayer midplane (i.e., the minimal surface), but the neutral plane of the membrane has a constant nonzero mean curvature because it has a fixed distance from the minimal surface (Anderson et al., 1988; Gruner, 1989). Because $H = K = 0$ in the L_α phase,

$$\Delta\mu_{curv} = 2\kappa\{\langle H - H_0\rangle^2 - H_0^2\} + \kappa_G\langle K\rangle. \qquad (3)$$

Because $H_o < H < 0$ for these nonbilayer membranes, Eq. 3 shows that $\Delta\mu_{curv}$ is always negative ($\Delta\mu_{curv} < 0$), and therefore, is an important factor stabilizing the nonbilayer phases. In contrast, in the H_{II} phase, alkyl chains of lipids have to extend to different lengths to fill the interstitial hydrocarbon region, which reduces the entropy of chains, and thereby, the free energy of the membrane increases (Anderson et al., 1988). This situation is almost the same in the cubic phases. Therefore, this packing energy of the alkyl chains unstabilizes the nonbilayer phases, and thus $\Delta\mu_{ch}$ is always positive ($\Delta\mu_{ch} > 0$). In most cases, phase transitions between the nonbilayer phases and the L_α phases are determined by the interplay of these two factors, $\Delta\mu_{curv}$ and $\Delta\mu_{ch}$. Eq. 3 shows that $|\Delta\mu_{curv}|$ decreases with a decrease in $|H_o|$.

For the MO membrane, $|H_o|$ is large and $\Delta\mu_{curv}$ has a large negative value. Therefore, $\Delta\mu < 0$, indicates that the cubic phase is stable. As the electrostatic interactions increase owing to the charged DOPA, $|H_o|$ of the membrane decreases, inducing the decrease in $|\Delta\mu_{curv}|$. At the critical value of the electrostatic interactions, $\Delta\mu = 0$, and thereby the cubic-to-L_α phase transition occurs. Above the critical value of the electrostatic interactions, $\Delta\mu > 0$ and thereby the L_α phase is stable. Hence, the decrease in$|H_o|$ with an increase in the electrostatic interactions induces the cubic-to-L_α phase transition in the DOPA/MO membrane.

Cubic phases are considered to play important roles in biological membranes in cells (Luzzati, 1997; Landh, 1995; Hyde et al., 1997). Three-dimensional regular structures of biomembranes similar to cubic phases have been often observed in various cells by transmission electron microscopy (TEM) (Hyde et al., 1997). The prolamellar body (PLB) in plant cells is one of the most famous examples. When plants are grown in the dark, etioplasts are formed in their leaf cells. These etioplasts change their structures and transform into chloroplasts after they are exposed to light. Therefore, they are considered to be at a pre-stage to form chloroplasts in normal development (Staehelin, 1986; Lütz, 1986). The characteristic structure in the etioplasts is a paracrystalline-like structure or a three-dimensional tubular lattice, called as PLB. It is often observed by TEM that the PLB is connected (or associated) with prothylakoids. After adsorbing light, the PLB transforms into the lamellae of thylakoids, which membranes are in the L_α phase. Immediately after the transformation, the membranes of the thy-

lakoids are not stacked and swelled in the chloroplast, then gradually stacked each other to form granas (Nishimura, 1987). The PLB structures have been considered as Q^{224} or Q^{229} phase based on the analysis of TEM, however its detailed structure remains unresolved (Hyde et al., 1997). What is the mechanism of biogenesis of the thylakoid from the PLB? The thylakoid is made of membranes in the L_α phase, but the membrane of the PLB is in the cubic phase, and thereby this transformation is considered as a kind of phase transition from the cubic phase to the L_α phase. Generally, the mechanism of the cubic-to-L_α phase transition is not well understood. In this report, we have proposed a new mechanism of the cubic-to-L_α phase transition, which may play an important role in the biogenesis of the thylakoid membrane from the PLB.

The effects of water contents on the phase stability of cubic phases have been vigorously investigated and reasonably explained by the curvature elastic energy (Turner et al., 1992; Templer et al., 1994; Chung and Caffrey, 1994b). However, the effects of electrostatic interactions due to the surface charge on the structure and stability of cubic phase membranes has never been investigated systematically. This report and our previous report (Aota-Nakano et al., 1999) have described the effects of the electrostatic interactions on the stability of cubic phases of the MO membrane, and the results can be reasonably explained qualitatively by the spontaneous curvature of membrane and the curvature elastic energy. Moreover, the experimental results in these reports clearly show that, as the electrostatic interactions decrease, $|H_o|$ increases, and the most stable phase of the lipid membrane changes as follows: $L_\alpha \Rightarrow Q^{229} \Rightarrow Q^{224} \Rightarrow H_{II}$. In the dispersion of didodecyl phosphatidylethanolamine (DPPE) in excess water, the phase sequence $L_\alpha \Rightarrow Q^{229} \Rightarrow Q^{224} \Rightarrow H_{II}$ was observed as temperature increased (Seddon et al., 1990). The molecular motion of the alkyl chain increases with an increase in temperature, so $|H_o|$ may increase. In the stability of cubic phases of lipid membrane, the increase in the electrostatic interactions due to the surface charge may have the similar effect as the decrease in temperature has. Therefore, we can conclude that the electrostatic interactions described in this report are another important method to control the stability of cubic phases and temperature. A more quantitative analysis of the effects of the electrostatic interactions on the cubic phase stability is necessary as a next step, and is in progress in our laboratory.

This work was supported partly by a grant from the Asahi Glass foundation, Japan (to M.Y.). We appreciate Dr. Caffrey and Elsevier Science for allowing us to use the figure in Qiu and Caffrey (2000) as the Fig. 1 in this report.

REFERENCES

Ai, X., and M. Caffrey. 2000. Membrane protein crystallization in lipidic mesophases: detergent effects. *Biophys. J.* 79:394–405.

Anderson, D. M., S. M. Gruner, and S. Leibler. 1988. Geometrical aspects of the frustration in the cubic phases of lyotropic liquid crystals. *Proc. Natl. Acad. Sci. U.S.A.* 85:5364–5368.

Andersson, S., S. T. Hyde, K. Larsson, and S. Lidin. 1988. Minimal surfaces and structures: from inorganic and metal crystals to cell membranes and biopolymers. *Chem. Rev.* 88:221–242.

Aota-Nakano, Y., S. J. Li, and M. Yamazaki. 1999. Effects of electrostatic interaction on the phase stability and structures of cubic phases of monoolein/oleic acid mixture membranes. *Biochim. Biophys. Acta.* 1461:96–102.

Basáñez, G., J. L. Nieva, E. Rivas, A. Alonso, and F. M. Goñi. 1996. Diacylglycerol and the promotion of lamellar-hexagonal and lamellar-isotropic phase transitions in lipids: implications for membrane fusion. *Biophys. J.* 70:2299–2306.

Briggs, J., H. Chung, and M. Caffrey. 1996. The temperature-composition phase diagram and mesophase structure characterization of the monoolein/water system. *J. Phys. II France.* 6:723–751.

Caffrey, M. 1987. Kinetics and mechanism of transitions involving the lamellar, cubic, inverted hexagonal, and fluid isotropic phases of hydrated monoacylglycerides monitored by time-resolved x-ray diffraction. *Biochemistry.* 26:6349–6363.

Chen, Z., and R. P. Rand. 1997. The influence of cholesterol on phospholipid membrane curvature and bending elasticity. *Biophys. J.* 73: 267–276.

Chen, Z., and R. P. Rand. 1998. Comparative study of the effects of several n-alkanes on phospholipid hexagonal phases. *Biophys. J.* 74:944–952.

Chung, H., and M. Caffrey. 1994a. The neutral area surface of the cubic mesophase: location and properties. *Biophys. J.* 66:377–381.

Chung, H., and M. Caffrey. 1994b. The curvature elastic-energy function of the lipid–water cubic mesophase. *Nature.* 368:224–226.

Colotto, A., and R. P. Epand. 1997. Structural study of the relationship between the rate of membrane fusion and the ability of the fusion peptide of influenza virus to perturb bilayers. *Biochemistry*. 36:7644–7651.

Colotto, A., I. Martin, J.-M. Ruysschaert, A. Sen, S. W. Hui, and R. P. Epand. 1996. Structural study of the interaction between the SIV fusion peptide and model membranes. *Biochemistry*. 35:980–989.

Czeslik, C., R. Winter, G. Rapp, and K. Bartels. 1995. Temperature- and pressure-dependent phase behavior of monoacylglycerides monoolein and monoelaidin. *Biophys. J.* 68:1423–1429

de Kruijff, B. 1997. Lipids beyond the bilayer. *Nature*. 386:129–130.

Glatter, O., and O. Kratky, 1982. Small Angle X-ray Scattering. Academic Press, New York.

Gruner, S. M. 1985. Intrinsic curvature hypothesis for biomembrane lipid composition: a role for nonbilayer lipids. *Proc. Natl. Acad. Sci. U.S.A.* 82:3665–3669.

Gruner, S. M. 1989. Stability of lyotropic phases with curved interfaces. *J. Phys. Chem*. 93:7562–7570

Gruner, S. M., P. R. Cullis, M. J. Hope, and C. P. S. Tilcock. 1985. Lipid polymorphism: the molecular basis of nonbilayer phases. *Annu. Rev. Biophys. Biophys. Chem.* 14:211–238.

Furuike, S., V. G. Levadny, S. J. Li, and M. Yamazaki. 1999. Low pH induces an interdigitated gel to bilayer gel phase transition in dihexadecylphosphatidylcholine membrane. *Biophys. J.* 77:2015–2023.

Helfrich, W.1973. Elastic properties of lipid bilayers: theory and possible experiments. *Z. Naturforsch.* 28c:693–703.

Hyde, S., S. Andersson, K. Larsson, Z. Blum, T. Landh, and B.W. Ninham. 1997. The language of shape. Elsevier Science B.V., Amsterdam.

Hyde, S. T., S. Andersson, B. Ericsson, and K. Larsson. 1984. A cubic structure consisting of a lipid bilayer forming an infinite periodic minimum surface of the gyroid type in the glycerolmonooleat-water system. *Z. Kristallogr*. 168:213–219.

Kinoshita, K., S. J. Li, and M. Yamazaki. 2001. The mechanism of the stabilization of the hexagonal II (H_{II}) phase in phosphatidylethanolamine membranes in the presence of low concentrations of dimethylsulfoxide. *Eur. Biophys. J.* DOI 10.1007/s002490000127.

Landau, E. M., and J. P. Rosenbusch. 1996. Lipidic cubic phases: a novel concept for the crystallization of membrane proteins. *Proc. Natl. Acad. Sci. U.S.A.* 93:14532–14535.

Landh, T. 1995. From entangled membranes to eclectic morphologies: cubic membranes as subcellular space organizers. *FEBS Lett*. 369: 13–17.

Li, X-j., and M. Schick. 2000. Theory of lipid polymorphism: application to phosphatidylethanolamine and phosphatidylserine. *Biophys. J.* 78: 34–46.

Lindblom, G., and L. Rilfors. 1989. Cubic phases and isotropic structures formed by membrane lipids—possible biological relevance. *Biochim. Biophys. Acta.* 988:221–256.

Longley, W., and T. J. McIntosh. 1983. A bicontinuous tetrahedral structure in a liquid–crystalline lipid. *Nature.* 303:612–614.

Lütz, C. 1986. Prolamellar bodies. *In* Photosynthesis III—Photosynthetic Membranes and Light Harvesting Systems, (Encyclopedia of Plant Physiology, Vol.19). L. A. Staehelin and C. J. Arntzen, editors. Springer-Verlag, Berlin. 683–705.

Luzzati, V. 1997. Biological significance of lipid polymorphism: the cubic phases. *Curr. Opin. Struct. Biol.* 7:661–668.

Luzzati, V., H. Delacroix, A. Gulik, T. Gulik-Kryzwicki, P. Mariani, and R. Vargas. 1997. The cubic phases of lipids. *In* Lipid Polymorphism and Membrane Properties. R. Epand, editor. Academic Press. 3–24

Luzzati, V., A. Gulik, M. DeRosa, and A. Gambacorta. 1987. Lipids from *Sulfolobus solfataricus*, life at high temperature and the structure of membranes. *Chemica Scripta.* 27B:211–219.

Luzzati, V., and F. Husson. 1962. X-ray diffraction studies of lipid–water systems. *J. Cell. Biol.* 12:207–219

Mariani, P., V. Luzzati, and H. Delacroix. 1988. Cubic phases of lipid-containing systems—structure analysis and biological implications. *J. Mol. Biol.* 204:165–189.

Marsh, D. 1996. Intrinsic curvature in normal and inverted lipid structures and in membranes. *Biophys. J.* 70:2248–2255.

Nishimura, M. 1987. Photosynthesis (in Japanese). Iwanami.

Pebay-Peyroula, E., G. Rummel, J. P. Rosenbusch, and E. M. Landau. 1997. X-ray structure of bacteriorhodopsin at 2.5 Angstroms from microcrystals grown in lipidic cubic phases. *Science*. 277:1676–1681.

Qiu, H., and M. Caffrey. 2000. The phase diagram of the monoolein/water system: metastability and equilibrium aspects. *Biomaterials.* 21:223–23.

Rand, R.P., and N.L. Fuller. 1994. Structural dimensions and their changes in reentrant hexagonal-lamellar transition of phospholipids. *Biophys. J.* 66:2127–2138.

Rand, R. P., N. L. Fuller, S. M. Gruner, and V. A. Parsegian. 1990. Membrane curvature, lipid segregation, and structural transition for phospholipids under dual-solvent stress. *Biochemistry.* 29:76–87.

Rummel, G., A. Hardmeyer, C. Widmer, M. L. Chiu, P. Nollert, K. P. Locher, I. Pedruzzi, E. M. Landau, and J. P. Rosenbusch. 1998. Lipid cubic phases: new matrices for the three-dimensional crystallization of membrane proteins. *J. Struct. Biol*. 121:82–91.

Seddon, J.M., J. L. Hogan, N. A. Warrender, and E. Pebay-Peyroula. 1990. Structural studies of phospholipid cubic phases. *Prog. Colloid Poly. Sci.* 81:189–197.

Seddon, J. M., and R. H. Templer. 1995. Polymorphism of lipid–water systems. *In* Structure and Dynamics of Membranes. R. Lipowsky and E. Sackmann, editors. Elsevier Science B. V., Amsterdam. 97–160.

Staehelin, L. A. 1986. Chloroplast structure and supramolecular organization of photosynthetic membranes. *In* Photosynthesis III—Photosynthetic Membranes and Light Harvesting Systems, (Encyclopedia of Plant Physiology, Vol.19). L. A. Staehelin and C. J. Arntzen, editors. Springer-Verlag. 1–84.

Templer, R. H., J. M. Seddon, and N. A. Warrender. 1994. Measuring the elastic parameters for inverse bicontinuous cubic phases. *Biophys. Chem.* 49:1–12.

Tenchov, B., R. Koynova, and G. Rapp. 1998. Accerated formation of cubic phases in phosphatidylethanolamine dispersions. *Biophys. J.* 75: 853–866.

Turner, D. C., Z.-G. Wanf, S. M. Gruner, D. A. Mannock, and R. M. McElhaney. 1992. Structural study of the inverted cubic phases of di-dodecyl alkyl β-D-glucopyranosyl-*rac*-glycerol. *J. Phys. II France.* 2:2039–2063.

Yamazaki, M., M. Ohshika, N. Kashiwagi, and T. Asano. 1992. Phase transition of phospholipid vesicles under osmotic stress and in the presence of ethylene glycol. *Biophys. Chem.* 43:29–37.